Incoherent Domain Configuration Along Wire Width in Permalloy Nanowires

Kyoung-Woong Moon[1], Jae-Chul Lee[1,2], Myung-Hwa Jung[3], Kyung-Ho Shin[2], and Sug-Bong Choe[1]

[1]Center for Subwavelength Optics and School of Physic and Astronomy, Seoul National University, Seoul 151-742, Republic of Korea

[2]Department of Physics, Sogang University, Seoul 121-742, Republic of Korea

[3]Nano-Device Research Center, Korea Institute of Science and Technology, Seoul 136-791, Republic of Korea

Magnetization reversal in ferromagnetic Permalloy nanowires is experimentally investigated by measurement of the anisotropic magnetoresistance (AMR). Two distinct regimes of the magnetization reversal are observed with respect to the angle of the external magnetic field. For the regime of large angles, the AMR curves exhibit two distinct jumps, evidencing the existence of an intermediate transient state. The intermediate state is in the form of an incoherent magnetization configuration consisting of three domain structures with two Néel walls, due to the inhomogeneous shape anisotropy distribution, as confirmed by a micromagnetic prediction.

***Index Terms*—Domain configuration, magnetization reversal, nanowire, permalloy.**

I. Introduction

MAGNETIZATION states and reversal processes in magnetic nanostructures are of increasing interest in recent years because of their potential applications to modern magnetoelectronic devices [1]–[4]. Among these nanostructures, the ferromagnetic nanowires have been intensively studied due to the possibility of prospective high density recording devices [5]–[9]. Several distinct mechanisms have been proposed for magnetization reversal in ferromagnetic nanostructures: coherent rotation [10], [11], curling [12], [13], buckling [14], and domain wall motion [15], depending on the geometries and the magnetic properties. The coherent rotation appears in structures smaller than the exchange length, in the form of a uniform magnetization rotating coherently. The curling and buckling modes occur in relatively large structures. These modes reduce the magnetostatic energy with costing the exchange energy. The curling mode forms spiral magnetization states in structures having a small aspect ratio, whereas the buckling mode appears in thin wires with wavy configuration of the magnetization along the wire. In the domain wall motion, the magnetization reversal is proceeded by domain expansion from nucleated cites.

In this study, we experimentally demonstrate that there exists another distinct mode in ferromagnetic nanowire structures. In the mode, the magnetization reverses first at the central region by creating two Néel walls to the edge regions, followed by the reversal at the edge regions with increasing an external magnetic field. The two jumps due to the reversals of the central and edge regions are detected by the AMR measurement.

II. Experiments

For this study, 5 nm Ti/20 nm Py/5 nm Ti films are deposited on oxidized Si substrates by dc-magnetron sputtering, followed by fabrication of nanowire structures via an e-beam lithography and ion milling techniques. The nanowire is 600-nm-wide and 17-μm-long, with tapered ends as depicted in Fig. 1. At both ends of the wire, gold electrodes are deposited for electrical transport measurement. An AMR measurement technique [16]–[18] is adopted to monitor the magnetization state of the ferromagnetic nanowires. The AMR is measured as the change of the electric resistivity with respect to the angle between the magnetization and the current. The AMR measurement technique provides a very sensitive probe to the magnetization state with high accuracy on the weak AMR signal intensity. For AMR measurement, the electric voltage between the electrodes with a constant dc current 100 μA is measured with sweeping the in-plane magnetic field at fixed angle φ to the wire as depicted in Fig. 1. All experiments are performed at room temperature.

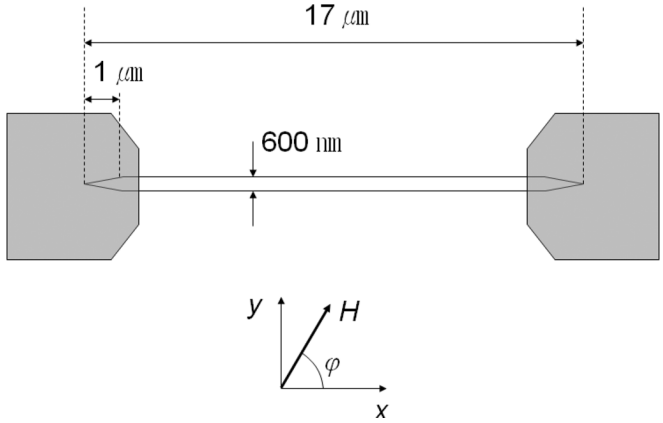

Fig. 1. Nanowire structure under examination and the measurement geometry.

III. Results and Discussion

Fig. 2 shows the measured AMR curves with respect to the external magnetic field for several angles as denoted in the figure. The AMR ratio is defined as $\Delta R/R_0 = (R(H) - R_0)/R_0$, where $R(H)$ is the electric resistance under an applied magnetic field H and R_0 is the resistance under zero field bias. Due

Manuscript received October 09, 2008. Current version published May 20, 2009. Corresponding author: S.-B. Choe (e-mail: sugbong@snu.ac.kr).

Color versions of one or more of the figures in this paper are available online at http://ieeexplore.ieee.org.

Digital Object Identifier 10.1109/TMAG.2009.2018666

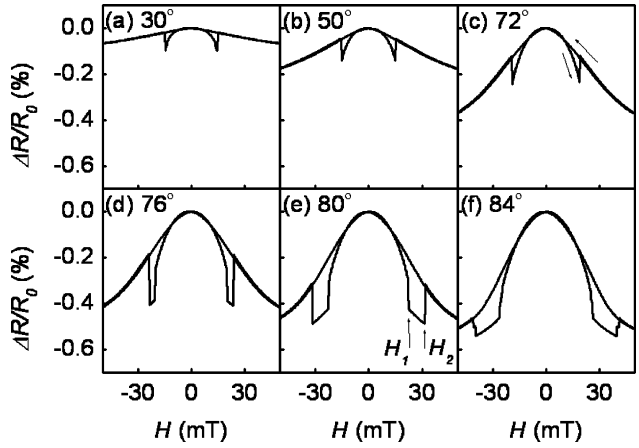

Fig. 2. Measured AMR curves of 600-nm-wide Permalloy wire at different angles φ as denoted in the figure.

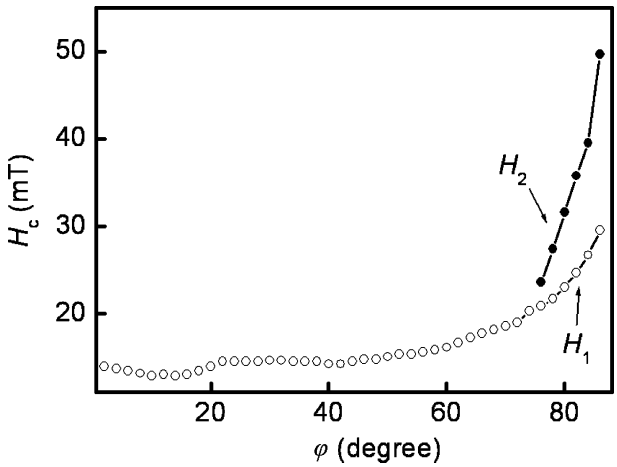

Fig. 3. Critical fields with respect to the angle φ.

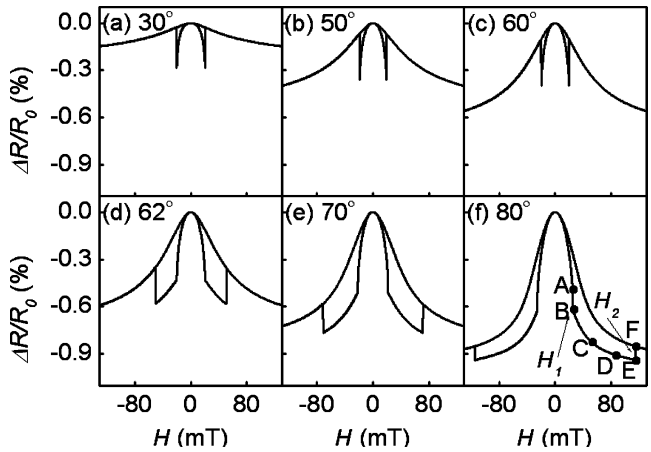

Fig. 4. Simulated AMR curves for different angles φ as denoted in the figure.

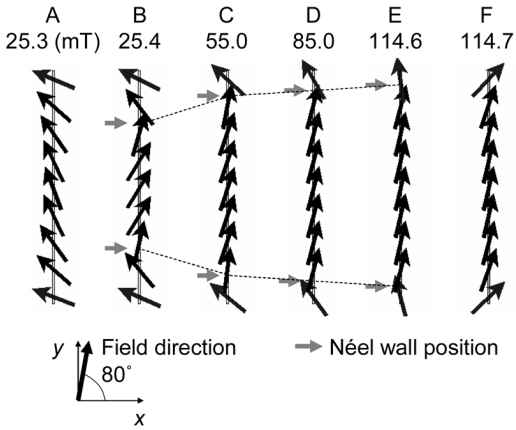

Fig. 5. Magnetization configuration along the wire width and Néel wall position with respect to the applied field denoted in the figure, as well as denoted by the points with corresponding labels in Fig. 4(f).

to the high signal-to-noise ratio of the AMR measurement, it is clearly seen in the figure that there exist two distinct reversal regimes with respect to the angle φ—a single jump in Figs. 2(a)–(c) and two jumps in Figs. 2(d)–(f).

In the first regime for $\varphi < 74°$, the reversal takes places by a single abrupt jump as shown in Fig. 2(a)–(c). There are several possible modes explaining this single jump—the coherent rotation [10], [11], curling [12], [13], and buckling [14] modes. Each particular reversal mode appears depending on the structure geometries as well as the magnetic properties. However, it is worthwhile to note that all the modes predict a single jump in the AMR curves. In contrary, two distinct jumps are observed from the AMR curves in the second regime for $\varphi > 74°$ as seen in Fig. 2(d)–(f).

The distinct regimes are again confirmed in Fig. 3, which plots the critical field with respect to the angle. The two jumps are bifurcated at 74° and the critical field H_1 and H_2 for each jump vary differently with increasing the angle.

To understand the origin of the two distinct regimes, a micromagnetic calculation is carried out by use of OOMMF [19] with periodic boundary condition [20]. The AMR curve is then reproduced by the relation between the AMR and the magnetization as $\Delta R/R_0 = -\Delta R_M \langle m_\perp \rangle^2$, where ΔR_M is the maximum AMR ratio and $\langle m_\perp \rangle$ is the averaged value of the direction cosine $m_\perp$ of the magnetization perpendicular to the current direction [17], [18]. The value of $\langle m_\perp \rangle$ is obtained from the micromagnetic calculation for every H with increment of 0.1 mT. The typical magnetic parameters of Permalloy are used in the simulation as the saturation magnetization $M_S = 8.6 \times 10^5$ A/m and the exchange constant $A_X = 1.3 \times 10^{-11}$ J/m. The damping constant is assumed to be 0.02.

The simulation results successfully reproduce the two distinct reversal behavior with a single jump and two jumps with respect to the angle of the magnetic field. Fig. 4 shows AMR curves predicted by the micromagnetic simulation for different angles φ.

The most intriguing question is how the two jumps in the AMR curves occur. To answer the question, we look into the detailed magnetization configurations between the two jumps. Fig. 5 shows the simulated results for the transient states between the two jumps. The arrows indicate the orientation of the local magnetization vector along the wire width. The magnetization profiles are calculated for 80° with varying the external magnetic field as denoted in the figure, as well as denoted by the points with corresponding labels in Fig. 4(f).

The nanowire exhibits an incoherent magnetization under a magnetic field smaller than H_1, as shown in Fig. 5(A). With increasing the field larger than H_1, the magnetization at the central

region reverses first while the local magnetization at the edge regions remains unreversed. It thus forms three domain states with two Néel walls [21] as shown in Fig. 5(B). The first jump in AMR curve corresponds to this reversal process of the central region. With further increment of the external field, the central domain expands outward as shown in Figs. 5(C)–(E). Finally, the edge domains reverse at H_2 as seen in Fig. 5(F), generating the second jump in AMR curve. The two jumps in AMR curve as seen in Fig. 4(d)–(f) thus correspond to the magnetization reversal of the central and edge regions, respectively.

The incoherent magnetization configuration is ascribed to the inhomogeneous shape anisotropy distribution. The magnetization at the edges of the wire structure generates the edge surface magnetization, whose density is proportional to the direction cosine of the magnetization normal to the wire edge. Since the surface magnetization produces the magnetostatic field and in consequence increases the magnetostatic energy, the local magnetization at the edges experiences additional effective shape anisotropy parallel to the wire. On contrary, the local magnetization at the central region is relatively free from the shape anisotropy. It is therefore natural to expect that the magnetization incoherently responds to the external magnetic field. The magnetization at the central region is relatively easy to rotate with respect to the external magnetic field, while the magnetization at the edge is fixed with the local shape anisotropy.

The angle 74° in the experiments is determined by the competition between magnetic energies. The central region magnetization reversed state reduces the Zeeman energy. However, nucleated two Néel walls increase the exchange energy and the magnetostatic energy. When the angle is smaller than 74°, the Zeeman energy reduction by the central region reversed to the field direction is not sufficiently large to overcome the increment of the exchange energy and the magnetostatic energy. When the angle is larger than 74°, the Zeeman energy reduction is larger than the increment of the exchange energy and the magnetostatic energy. So, the central region reversed state is formed with stability.

The reversal regime of two jumps disappears for nanowires narrower than 400 nm, as observed from the experimental measurement on the nanowires with the widths 130, 230, 330, 440, and 600 nm. However, the shapes of the AMR curves and the critical fields are better fit with the incoherent magnetization configuration, rather than the coherent magnetization configuration. Despite of the general presumption that the magnetization lies along the wire length direction in ferromagnetic nanowires, our results demonstrate that the magnetization is incoherent along the wire width direction and thus reversed locally.

IV. Conclusion

We experimentally investigate the incoherent magnetization reversal mode in ferromagnetic Permalloy nanowires. For external magnetic field applied at a large angle to the nanowires, the AMR curves exhibit two distinct jumps for magnetization reversal. The two distinct jumps are ascribed to the formation of the intermediate incoherent magnetization state consisting of three domains along the wire width. The incoherent magnetization state is confirmed by a micromagnetic calculation.

Acknowledgment

This study was supported by the Korea Science and Engineering Foundation through the NRL program (R0A-2007-000-20032-0). The work of K.-W. Moon was supported by the Seoul R&BD Program.

References

[1] G. Prinz and K. Hathaway, "Magnetoelectronics-special issue," *Phys. Today*, vol. 48, no. 4, p. 24, Apr. 1995.
[2] D. A. Allwoode, G. Xiong, C. C. Faulkner, D. Atkinson, D. Petit, and R. P. Cowburn, "Magnetic domain-wall logic," *Science*, vol. 309, no. 5741, p. 1688, Sep. 2005.
[3] L. Sun, Y. Hao, C.-L. Chien, and P. C. Searson, "Tuning the properties of magnetic nanowires," *IBM J. Res. Dev.*, vol. 49, no. 1, p. 79, Jan. 2005.
[4] S. Tehrani, E. Chen, M. Durlam, M. DeHerrera, J. M. Slaughter, J. Shi, and G. Kerszykowski, "High density submicron magnetoresistive random access memory (invited)," *J. Appl. Phys.*, vol. 85, no. 8, p. 5822, 1999.
[5] M. Hayashi, L. Thomas, C. Rettner, R. Moriya, and S. S. P. Parkin, "Direct observation of the coherent precession of magnetic domain walls propagating along permalloy nanowires," *Nat. Phys.*, vol. 3, no. 1, p. 21, Jan. 2007.
[6] S. S. P. Parkin, M. Hayashi, and L. Thomas, "Magnetic domain-wall racetrack memory," *Science*, vol. 320, no. 5873, p. 190, Apr. 2008.
[7] L. Heyne, M. Kläui, D. Backes, T. A. Moore, S. Krzyk, U. Rüdiger, L. J. Heyderman, A. F. Rodríguez, F. Nolting, T. O. Mentes, M. Á. Niño, A. Locatelli, K. Kirsch, and R. Mattheis, "Relationship between nonadiabaticity and damping in permalloy studied by current induced spin structure transformations," *Phys. Rev. Lett.*, vol. 100, no. 6, p. 066603, Feb. 2008.
[8] A. Yamaguchi, T. Ono, S. Nasu, K. Miyake, K. Mibu, and T. Shinjo, "Real-space observation of current-driven domain wall motion in submicron magnetic wires," *Phys. Rev. Lett.*, vol. 92, no. 7, p. 077205, Feb. 2004.
[9] K.-J. Kim, J.-C. Lee, S.-B. Choe, and K.-H. Shin, "Joule heating in ferromagnetic nanowires: Prediction and observation," *Appl. Phys. Lett.*, vol. 92, no. 19, p. 192509, May 2008.
[10] Y. Jaccard, Ph. Guittienne, D. Kelly, J.-E. Wegrowe, and J.-Ph. Ansermet, "Uniform magnetization rotation in sigle ferromagnetic nanowires," *Phys. Rev. B*, vol. 62, no. 2, p. 1141, July 2000.
[11] Th. G. S. M. Rijks, S. K. J. Lenczowski, R. Coehoorn, and W. J. M. de Jonge, "In-plane and out-of-plane anisotropic magnetoresistance in $Ni_{80}Fe_{20}$ thin films," *Phys. Rev. B*, vol. 56, no. 1, p. 362, Jul. 1997.
[12] A. Aharoni, "Angular dependence of nucleation by curling in a prolate spheroid," *J. Appl. Phys.*, vol. 82, no. 3, p. 1281, Aug. 1997.
[13] T. Y. Chung and S. Y. Hsu, "Magnetization reversal in single domain Permalloy wires probed by magnetotransport," *J. Appl. Phys.*, vol. 103, no. 7, p. 07C506, Feb. 2008.
[14] A. B. Oliveira, S. M. Rezende, and A. Azevedo, "Magnetization reversal in permalloy ferromagnetic nanowires investigated with magnetoresistance measurements," *Phys. Rev. B*, vol. 78, no. 2, p. 024423, Jul. 2008.
[15] T. Ono, H. Miyajima, K. Shigeto, and T. Shinjo, "Magnetization reversal in submicron magnetic wire studied by using giant magnetoresistance effect," *Appl. Phys. Lett.*, vol. 72, no. 9, p. 1116, Mar. 1998.
[16] K. Hong and N. Giordano, "New effects in ferromagnetic nanostructures," *J. Magn. Magn. Mater.*, vol. 151, no. 3, p. 396, Dec. 1995.
[17] J.-E. Wegrowe, D. Kelly, A. Franck, S. E. Gilbert, and J.-Ph. Ansermet, "Magnetoresistance of ferromagnetic nanowires," *Phys. Rev. Lett.*, vol. 82, no. 18, p. 3681, May 1999.
[18] Th. G. S. M. Rijks, R. Coehoorn, M. J. M. de Jong, and W. J. M. de Jonge, "Semiclassical calculations of the anisotropic magnetoresistance of NiFe-based thin-films, wires and multilayers," *Phys. Rev. B*, vol. 51, p. 283, Jan. 1995.
[19] M. Donahue and D. Porter, "OOMMF," Oct. 30, 2000, (1.2a4 ver.) [Online]. Available: http://math.nist.gov/oommf/
[20] K. Lebecki, "OOMMF_PBC," Dec. 1, 2006, (1.2a4 ver.) [Online]. Available: http://info.ifpan.edu.pl/~lebecki/pbc.htm/
[21] N. Smith, "A specific model for domain-wall nucleation in thin-film Permalloy microelements (invited)," *J. Appl. Phys.*, vol. 63, no. 8, p. 2932, Apr. 1988.